# Efficient Termination of Cardiac Arrhythmias using Optogenetic Resonant Feedback Pacing

S. Hussaini,[1,2,3] A. Mamyraiym-Kyzy,[1] J. Schröder-Schetelig,[1,2,3] S.L. Lädke,[1] V. Venkatesan,[1] L. Diaz,[4,3] R.Q. Uribe,[1,3] C. Richter,[1,3,5] V.N. Biktashev,[6] R. Majumder,[1,2,3] V. Krinski,[1] and S. Luther*[1,2,3]

[1)] *Research Group Biomedical Physics, Max Planck Institute for Dynamics and Self-Organisation, Göttingen, 37077, Germany*

[2)] *Institute of Pharmacology and Toxicology, University Medical Center Göttingen, 37075, Germany*

[3)] *DZHK (German Center for Cardiovascular Research), Partner Site Göttingen, 37075, Germany*

[4)] *Research Electronic Department, Max Planck Institute for Dynamics and Self-Organisation, Göttingen, 37077, Germany*

[5)] *WG Cardiovascular Optogenetics, Lab Animal Science Unit, Leibniz Institute for Primate research, Göttingen, 37077, Germany*

[6)] *Mathematics and Statistics Department, University of Exeter, EX4 4QF, UK*

(*Electronic mail: stefan.luther@ds.mpg.de)

(Dated: 3 January 2024)

Malignant cardiac tachyarrhythmias are associated with complex spatio-temporal excitation of the heart. The termination of these life-threatening arrhythmias require high-energy electrical shocks that have significant side effects, including tissue damage, excruciating pain, and worsening prognosis. This significant medical need has motivated the search for alternative approaches that mitigate the side effects, based on a comprehensive understanding of the nonlinear dynamics of the heart. Cardiac optogenetics enables the manipulation of cellular function using light, enhancing our understanding of nonlinear cardiac function and control. Here, we investigate the efficacy of optically resonant feedback pacing ($O_{RFP}$) to terminate ventricular tachyarrhythmias using numerical simulations and experiments in transgenic Langendorff-perfused mouse hearts. We show that $O_{RFP}$ outperforms the termination efficacy of optical single-pulse ($O_{SP}$) approach. At a termination rate of 50%, $O_{RFP}$ requires two orders of magnitude less light intensity per pulse than $O_{SP}$. We demonstrate that even at light intensities below the excitation threshold, $O_{RFP}$ enables the termination of arrhythmias by spatio-temporal modulation of excitability inducing spiral wave drift.

**Sudden cardiac death and arrhythmias account for about 15-20% of annual deaths worldwide[1]. Two of its important precursors are ventricular tachycardia (VT) and ventricular fibrillation (VF). These occur when the heart begins to deliver impulses irregularly and incoherently, impairing its efficient and coordinated pumping action. Without medical intervention, survival time is limited to minutes. Therefore, patients with VT or VF are treated with electroshock therapy, which can be administered externally or internally. Patients at high risk for these disorders are often advised to use implantable cardioverter defibrillators (ICDs) which continuously monitor the heart rate and deliver electrical shocks to the heart when the beating rate is outside the physiologically acceptable range. Despite high success rate, ICD therapy is associated with significant side effects, such as tissue damage, traumatic pain and psychological disturbances. Therefore, there is medical need for the development of low-energy arrhythmia therapy that overcome the common drawbacks and help to address the risk of cardiac arrhythmias.**

## I. INTRODUCTION

Self-organised pattern formation in an excitable reaction-diffusion system with nonlinear local dynamics is studied in a wide range of applications: chemical media such as the Belousov-Zhabotinsky (BZ) reaction system and biological media such as the heart[2,3]. Rotating spiral/scroll waves (a typical pattern in excitable media) in the heart are associated with life-threatening cardiac tachyarrhythmias such as ventricular tachycardia (VT) and ventricular fibrillation (VF) [4–6]. The termination of these arrhythmias require to apply a high-voltage shock that resets all electrical activity in the heart, allowing normal cardiac rhythm to resume. However, despite its high efficiency, this electrical defibrillation entails detrimental side effects, including traumatic pain, tissue damage, and worsensing of prognosis, which strongly motivate the search for alternative low-energy defibrillation techniques[7,8].

In contrast to globally resetting high-energy shocks, low-energy defibrillation approaches aim to control the nonlinear dynamics of spiral and scroll waves underlying the arrhythmias. Theoretical and numerical studies demonstrate the potential of resonant drift induced by low-amplitude global pacing at the spiral rotation frequency to control and terminate cardiac arrhythmias. In 1987 Davydov *et al.*[9] presented the first analytical study of resonant spiral drift, a phenomenon which was demonstrated by Agladze *et al.*[10] in experiments of the BZ reaction system. Biktashev and Holden[11] proposed

to add feedback to the pacing. It is aimed to maintain resonance when the spiral drifts in the heterogeneous cardiac muscle. It resulted in the robustness of the induced drift of the spiral wave and its termination in theory and numerical models. Although this concept has been extensively investigated in theory [11–15], and in some experiments[16,17], its potential as a low-energy alternative anti-arrhythmic technique has not yet been fully explored.

Cardiac optogenetics is a technique which allows normally light-insensitive cardiac tissue to become sensitive to light stimuli by genetic modification. The altered tissue then responds to light pulses by an increase or decrease of the transmembrane voltage of its cells, resulting in modulation of its excitability, or by assisting the propagation of excitation waves. Previous studies have demonstrated the potential of optogenetics to control electrical spiral waves in the heart with high spatio-temporal resolution[18–20]. In particular, the termination of arrhythmias was demonstrated using sub-threshold [21–23], as well as supra-threshold optical stimulation[24–29]. Sub-threshold optical stimulation increases cell membrane voltage below the excitation threshold (minimum membrane voltage required to excite the cell) resulting only in a change in excitability and does not trigger an excitation. In contrast, supra-threshold optical stimulation raises the cell membrane voltage above the threshold, leading to the onset of an action potential and the propagating of an excitation wave.

Clinical translation of optogenetics faces major challenges, such as off-target gene expression, immune responses that lead to impairment of long-term gene expression, and light delivery to the target tissue[30–33]. Overcoming these limitations may require a longer period of time, but improving pacing protocols to achieve high termination efficacy is another challenge that can be addressed in the interim. To this end, computational studies and available optogenetically modified animal models are excellent tools to address this particular challenge.

Here, we use cardiac optogenetics to study and control the dynamics of arrhythmia intact Langendorff-perfused transgenic mouse hearts. For this purpose, we use two pacing protocols: I) optical resonant feedback pacing $O_{RFP}$ and II) optical single pulse $O_{SP}$. Our results show, at a termination rate of 50%, $O_{RFP}$ requires two orders of magnitude less light intensity per pulse than $O_{SP}$. Furthermore, we demonstrate that $O_{RFP}$ enables termination of arrhythmias even at sub-threshold intensities. To elucidate the possible mechanism of arrhythmia termination, we performed 2-dimensional numerical simulations on genetically modified mouse ventricular tissue. We illustrate that resonant global sub-threshold illumination leads to spatiotemporal modulation of cardiac tissue excitability, causing the spiral wave to drift and terminate by colliding with nonexcitable boundaries. Therefore, resonant drift of the spiral wave could be the main mechanism for arrhythmia termination during $O_{RFP}$.

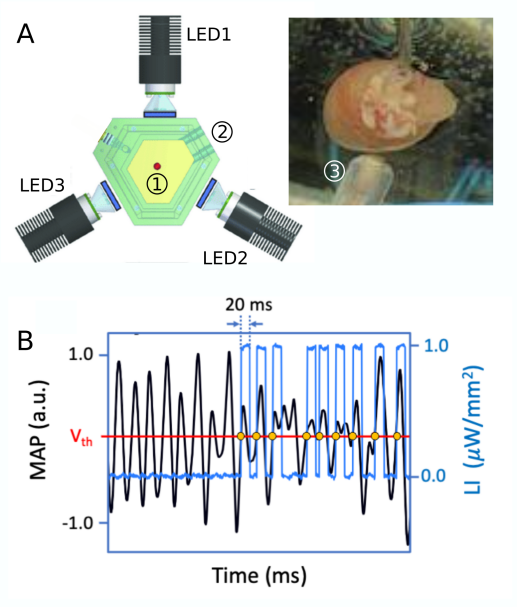


FIG. 1. Experimental setup. A) Langendorff-perfused transgeneic mouse heart (1) in temperature controlled bath (2). LED $1-3$ positioned at $0°$, $120°$, and $240°$ illuminate of the entire epicardium. Monophasic action potential (MAP) electrode (3) is positioned on left ventrincle. B) Normalized MAP signal (black) during ventricular arrhythmia. Increase of MAP signal above voltage threshold $V_{th}$ (red) triggers light pulse (blue) with light intensity $40\,\mu W/mm^2$, pulse length 20 ms.

## II. METHODS

The experiments were performed in accordance with the German Animal Welfare Act and declared to our animal welfare officers; the application for approval of animal experiments was authorized by the responsible animal welfare office (Lower Saxony State Office for Consumer Protection and Food Safety). Humane welfare-oriented procedures were implemented in agreement with the Guide for the Care and Use of Laboratory Animals and the recommendations of the Federation of Laboratory Animal Science Associations (FELASA).

### A. Experiments

In experiments, Langendorff-perfused $\alpha$-MHC-ChR2 transgenic mouse hearts with channelrhodopsin-2 (ChR2) expression restricted to cardiomyocytes were used. Tyrode solution (130 mM NaCl, 4 mM KCl, 1 mM $MgCl_2$, 24 mM $NaHCO_3$, 1.8 mM $CaCl_2$, 1.2 mM $KH_2PO_4$, 5.6 mM glucose, 1% albumin/BSA aerated with carbogen [95% $O_2$ and 5% $CO_2$]) was used to maintain the normal electrophysiological state of the heart during perfusion. All experiments were conducted at $37\,°C$. To induce arrhythmias, a sequence of 30 electrical pulses (amplitude $2.3\,V - 2.5\,V$, pulse duration $1\,ms - 3\,ms$) and frequencies $30\,Hz - 50\,Hz$ was applied the ventricles using a needle electrode. Sustained tachyarrhyth-

mias were ensured by reducing the KCl concentration in the Tyrode solution from 4 mM to 2 mM and by adding 100 µM pinacidil (a KATP channel activator) to the Tyrode. The hearts were globally illuminated as shown in Fig 1-A, using 3 LEDs ($\lambda = 470$ nm) positioned at 0°, 120°, and 240° surrounding the bath. For further details, we refer to Uribe *et al.*[28].

Pacing protocol $O_{RFP}$ was applied to N = 5 mouse hearts to control ventricular arrhythmias. $O_{RFP}$ consists of a series of triggered light pulses with a pulse length (PL) of 20 ms and light intensity (LI) within the range of 3.1 to 103.5 $\mu W/mm^2$. As it's shown in Fig. 1-B during $O_{RFP}$ the optical pulses were triggered if the monophasic action potential (MAP) signal exceeds the threshold signal $V_{th} = 0$ a u until the arrhythmias was terminated or after reaching the maximum duration of 10 s after the first trigger event. Arrhythmia termination was detected if the dominant frequency decreased below 5 Hz.

For each heart, the optical stimulation threshold was determined. In sinus rhythm the heart was paced with 10 pulses (with a frequency two times faster than sinus rhythm's rate) with a pulse width of 20 ms duration and increasing light intensity until capture was observed in the MAP signal. We performed $5-10$ arrhythmia termination attempts for each light intensity and pulse length. If unsuccessful, high-intensity global illumination was applied to terminate the arrhythmia. Between each trial, the heart was allowed to recover and rest for 60 s. Experiments were terminated if heart rate in sinus rhythm decreased below 3 Hz. For comparison, pacing protocol $O_{SP}$ with a LI from 4.5 to 1160 $\mu W/mm^2$ and PLs of 10 and 100 ms was applied to N = 5 mouse hearts.

### B. Numerical Simulations

To describe the electrical activity in the mouse heart ventricle, we used the modified version of the Bondarenko model[34,35]. This model contains 40 ordinary differential equations solved by Runge-Kutta (4th order) method with time step of $10^{-4}$ ms. The time evolution of the membrane voltage is as follows:

$$\frac{\partial V}{\partial t} = \nabla . \mathscr{D} \nabla V - \frac{\Sigma I_{ion} + I_{stim}}{C_m}. \quad (1)$$

$$\Sigma I_{ion} = I_{Ktof} + I_{Ktos} + I_{Kr} + I_{Kur} + I_{Kss} + I_{K1} + I_{Ks} + I_{Na^+} + I_{Ca} + I_{NaCa} + I_{Ca} + I_{NaK} + I_{CaCl} + I_{Nab} + I_{Cab}. \quad (2)$$

In Eq 1, $C_m$ = 1.0 $\mu F/cm^2$ is the specific capacitance of a cell membrane, $\mathscr{D}$ = 0.000 14 $cm^2/ms$ is the diffusion coefficient, which accounts for interacellular coupling, and is responsible for setting the conduction velocity of a propagating plane wave to 43.9 cm/s. $I_{ion}$ is the total ionic current, composed of the rapidly recovering transient outward $K^+$ current ($I_{Ktof}$), the slowly recovering transient outward $K^+$ current ($I_{Ktos}$), the rapid delayed rectifier $K^+$ current ($I_{Kr}$), the ultrarapidly activation delayed rectifier $K^+$ current ($I_{Kur}$), the noninactivating steady-state voltage-activated $K^+$ current ($I_{Kss}$), the time-independent inwardly rectifying $K^+$ current ($I_{K1}$), the slow delayed rectifier $K^+$ current ($I_{Ks}$), the fast $Na^+$ current ($I_{Na}$), the L-type $Ca^{2+}$ current ($I_{Ca}$) , $Na^+/Ca^{2+}$ exchange current ($I_{NaCa}$), the $Ca^{2+}$ pump current ($I_{Ca}$), the $Na^+/K^+$ pump current ($I_{NaK}$), the $Ca^{2+}$ activated $Cl^-$ current ($I_{CaCl}$), the background $Na^+$ current ($I_{Nab}$) and the background $Ca^{2+}$ current ($I_{Cab}$). $I_{stim}$ is the extra transmembrane current caused by an external stimulus.

To incorporate light sensitivity, the model was coupled with a 4-state mathematical model of a light-gated protein (Channelrhodopsin-2 or ChR2)[36] which responds to blue light stimuli (wavelength 470 nm), to produce a current ($I_{ChR2}$) as follows:

$$I_{ChR2} = g_{ChR2}\, G(V)(O_1 + \gamma O_2)(V - E_{ChR2}) \quad (3)$$

$$G(V) = [(10.6408 - 14.6408 \times exp(-V/42.7671))]/(4) \quad (4)$$

$$dC_1/dt = G_r C_2 + G_{d1} O_1 - k_1 C_1 \quad (5)$$

$$dO_1/dt = k_1 C_1 - (G_{d1} + e_{12}) O1 + e_{21} O_2 \quad (6)$$

$$dC_2/dt = G_{d2} O_2 - (k_2 + G_r) C_2 \quad (7)$$

$$dO_2/dt = k_2 C_2 - (G_{d2} + e_{21}) O_2 + e_{12} O_1 \quad (8)$$

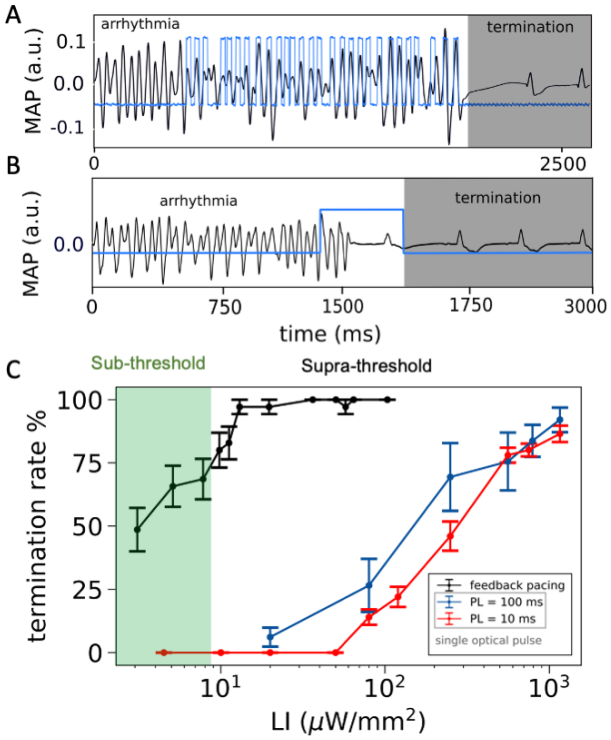


FIG. 2. Terminating efficacy of ventricular tachyarrhythmias. A) arrhythmia termination using optical resonant feedback pacing ($O_{RFP}$). Monophasic action potential (MAP, black) and light intensity (LI, blue) triggered from MAP time series result in arrhythmia termination (gray). B) arrhythmia termination using optical single pulse ($O_{SP}$) (pulse length (PL) 100 ms, LI = 560 $\mu W/mm^2$ ). C) arrhythmia termination efficacy in mouse hearts (N = 5) vs. LI for $O_{RFP}$ (black line) and $O_{SP}$ (blue line: PL 100 ms, red line: PL 10 ms). Green shaded area indicates sub-threshold LI, data given in mean ± SEM.

Here $g_{ChR2}$ is the maximum conductance, G(V) is the voltage-dependent rectification function, $O_1$ and $O_2$ are the open states of ChR2, $\gamma = 0.1$ is, probability, the ratio of contribution of the open states $O_2/O_1$, $V$ is the membrane voltage, and $E_{ChR2}$ is the reversal potential, which was taken to be 0 mV. $G_1$, $G_{d1}$, $G_{d2}$, $e_{12}$, $e_{21}$, $k_1$ and $k_2$ are the kinetic parameters corresponding to the transition states of ChR2 states (close: $C_1$, $C_2$; open: $O_1$, $O_2$). The model parameters are described in Ref[36]. To stimulate the cell membrane optically, $I_{ChR2}$ is used as $I_{stim}$ in Eq 1.

We integrate Eqs1-8 in a 2D domain of size $25 \times 25$ mm$^2$ with dx = dy = 0.025 cm and using finite difference method with five-point stencil. Then, we induced a single spiral wave in the domain detailed in Ref.[21]. To control the spiral wave dynamics, we apply the $O_{SP}$ and $O_{RFP}$ protocols. With $O_{RFP}$, we applied a sequence of pulses with a width of 33 ms (half of the spiral wave period 66 ms) each starting at $V_{th} = -40$ mV during depolarisation. We use N = 25 initial conditions to test termination efficacy for each LI. For each initial conditions, have induced the spiral wave in such a way that the tip of the spiral wave is positioned at different points in the domain.

## III. RESULTS

Fig. 2A shows a MAP signal (black) obtained during a VT in a Langendorff-perfused optogenetic mouse heart. During $O_{RFP}$, the MAP signal triggers a pulsed, global illumination (shown in a blue trace) of the entire epicardium (PL = 20 ms, LI = 40 $\mu$W/mm$^2$) when the signal amplitude rises above the trigger level. In this example, it requires n = 27 light pulses over a period of about 1.4 seconds, to terminate the arrhythmia allowing sinus rhythm to resume. For comparison, Fig. 2B shows the successful termination of an arrhythmia using the protocol $O_{SP}$ with PL = 100 ms and LI = 560 $\mu$W/mm$^2$. Following the onset of the light pulse, the arrhythmia is terminated following a short transient and the heart returns to sinus rhythm. The termination of arrhythmia is a stochastic process, where the success rate (SR) of each protocol depends on the LI, as shown in Fig. 2C. For $O_{SP}$, the termination efficacy increases with increasing LI, with longer PL result in increased efficacy. The LIs resulting in 50% and 75% SR, $LI_{50}$ and $LI_{75}$, are 150 and 560 $\mu$W/mm$^2$, respectively. Also SR of $O_{RFP}$ method increases monotonically with LI. However, in contrast to $O_{SP}$, for $O_{RFP}$, $LI_{50}$ is at 3.1 $\mu$W/mm$^2$, whereas $LI_{75}$ is 9.8 $\mu$W/mm$^2$. Thus, $O_{RFP}$ requires 50 fold less LI to obtain 50% SR, 56 fold less intensity to a 75% SR.

In $O_{RFP}$ method, light pulses are triggered until the arrhythmia is terminated or the maximum duration of the sequence has been reached (10 s). Fig. 3A shows that the number of pulses (PL = 20 ms) required to successfully terminate the arrhythmia decreases with increasing LI, from a mean of $40-50$ pulses at 1.3 $\mu$W/mm$^2$ to $1-2$ pulses at 103.5 $\mu$W/mm$^2$. Correspondingly, the total time to termination decreases with increasing LI from $1-2$ s to 0.1 s (Fig. 3B). It is also noteworthy that the termination time for $O_{SP}$ is about 100 ms. For $O_{RFP}$, the total energy required for termination, i.e. the energy summed over all pulses of the sequence, remains essentially

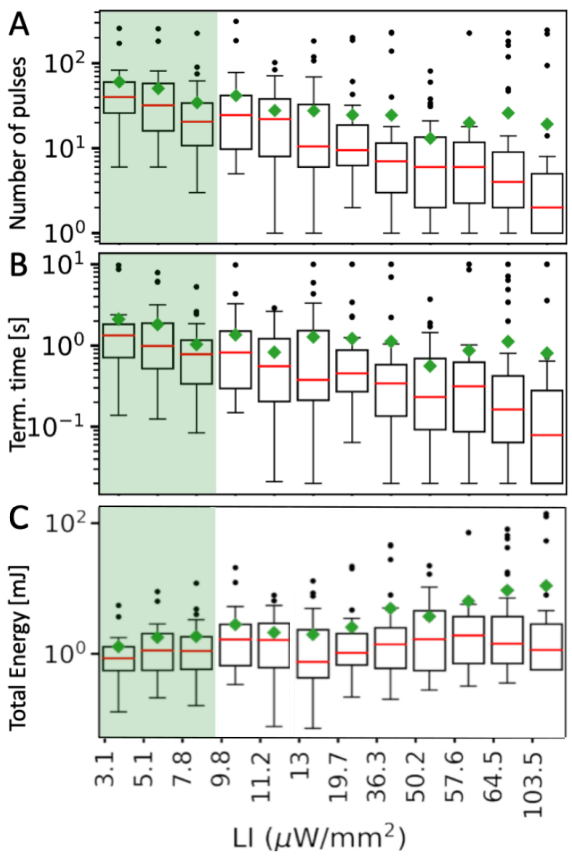


FIG. 3. Number of pulses (NPs), termination times, and total energy for successful termination of tachyarrhythmias using resonant feedback pacing. A) Nps with pulse length 20 ms. B) Termination times. C) Total energy of the pulse sequence. Boxplots indicate median (green diamond), mean (red line), and outlier (black circle), green shaded boxes indicate the sub-threshold regime.

constant at 1 mJ (Fig. 3C) in our experiments. In comparison, the energy for $O_{SP}$ at 50% success rate is 0.035 mJ for PL of 10 ms and 0.21 mJ for PL of 100 ms. In addition, we calculated the energy per pulse at a success rate of 50% ($E_{50}$) and found that 40 times more energy is required at a PL of 10 ms and 240 times more energy is required at a PL of 100 ms compared with $O_{RFP}$. All these details are summarized in table I along with the number of pulses (NP) required at 50%, 75%, and 100% termination rates for each of the $O_{SP}$ and $O_{RFP}$ methods. Using numerical simulations, we investigate possible mechanisms underlying the termination of spiral waves (SWs) by $O_{RFP}$, especially at LIs below the excitation threshold. Fig. 4A shows a counterclockwise rotating SW with a circular core. The time series shown in Fig. 4E represents the electrical activity of the domain recorded by the measuring electrode (indicated by a red dot). During $O_{RFP}$, the time series triggers a sequence of global light pulses with a subthreshold LI = 20 $\mu$W/mm$^2$ and PL = 33 ms. As a result, $O_{RFP}$ induces the drift of the SW, which finally collides with the boundary after NP = 9 (Fig. 4C-D).

We repeat this numerical experiment for N = 25 initial con-

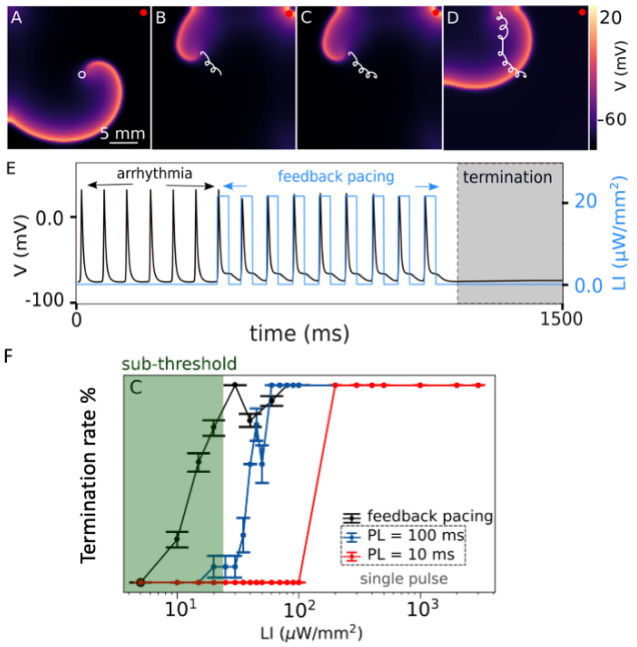


FIG. 4. Spiral wave (SW) termination *in silico*. A) The SW rotates with an initially circular core. (B), (C), and (D) illustrate the drift of the SW during optical resonant feedback pacing ($O_{RFP}$). E) Electrical activity (black) of the domain recorded by a measuring electrode (red dot). Blue trace shows optical pulses.Grey shaded box indicates the SW termination. F) Termination efficacy of SWs (N = 5) vs. light intensity (LI) for $O_{RFP}$ (black line) and and optical single pulse (blue line: PL 100 ms, red line: PL 10 ms). Green shaded area indicates sub-threshold LI, data given in mean ± SEM.

ditions and LI ranging from sub- to supra-threshold. Fig. 4E shows the resulting numerical dose-response curve, which qualitatively reproduces the experimental observations. In particular, we observe high termination efficiency at sub-threshold LIs for $O_{RFP}$. The SR varies between 0% and 75% for the LIs of 5...20 $\mu W/mm^2$. For supra-threshold LIs, the SR increases toward 100%. We therefore hypothesize that the drift induced by $O_{RFP}$ is a mechanism that contributes to the termination of VTs at sub-threshold LIs.

Fig. 5 shows a space-time representation of the dynamics of the SWa under the effect of $O_{RFP}$ at different LIs. The space-time diagrams show the membrane potential along a horizontal line in the 2D domain at y = 12.5 mm. We observe the termination of the waves due to drift at sub-threshold intensities, as well as supra-threshold intensities near the excitation threshold. At the supra-threshold regime with LI = 50 $\mu W/mm^2$, the termination of the SW is followed by the propagation of plane waves induced by illumination. However, at higher intensities, i.e., LI = 80 and 100 $\mu W/mm^2$, the rapid excitation of the entire region leads to phase resetting and termination of the SW. In the space-time plot, the core of the drifting SW is indicated by a dashed line. For a stationary SW, this line is vertical in the space-time representation. A drifting core is represented by an oblique line indicating the direction of motion and velocity (slope). As the LI increases, the drift velocity increases, corresponding to a

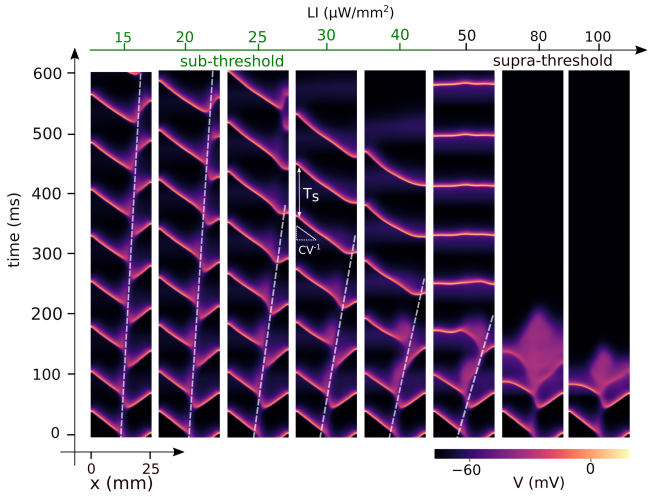


FIG. 5. Mechanisms for termination of a spiral wave during optical resonant feedback pacing ($O_{RFP}$). Space-time plots along a line of a 2-dimensional domain containing a spiral wave paced using $O_{RFP}$ method. The dashed line indicates the core region of the wave.

decreasing slope. In addition, an increment of LI leads to a longer rotation time of the SW (Ts) and a decrease of the conduction velocity (CV).

## IV. DISCUSSION

In this study, we have experimentally investigated the control of cardiac arrhythmias by resonant feedback pacing based on theoretical and numerical work by Davidov and co-workers [9,10] and Biktashev and Holden[11,37]. The latter introduced feedback to maintain resonant pacing conditions even when the spiral drifts in the presence of heterogeneities and boundaries. In their numerical study, Biktashev and Holden applied a global electric field pulse when the membrane potential at a local electrode exceeded a predefined threshold. This approach led to robust spiral drift and improved success rate in terminating single spiral waves in simulations. Furthermore, spiral/scroll wave termination using resonant pacing with feedback has been studied in 2D models and 3D simulations with realistic heart geometry[12,38–42]. However, the experimental implementation remained elusive. The present study uses global illumination to demonstrate the efficient termination of ventricular tachyarrhythmias in intact optogenetic mouse hearts by optical resonant feedback pacing (ORFP) at subthreshold and suprathreshold light intensities.

The experiments confirm the predicted higher termination effectiveness of resonant feedback stimulation compared to single pulses in terms of energy per pulse. However, the total energy requirement for a single pulse and pacing sequence remains comparable, as stimulation sequences with low intensities require an increasing number of pulses. Depending on the light intensity, duration, number, and timing of the pulses, various mechanisms that influence the dynamics of the spiral waves and contribute to their termination were

identified. When a single light pulse is applied, suprathreshold light intensities lead to tissue depolarization and wave termination with energy-dependent efficacy[18,28]. As a result of a suprathreshold light pulse, termination is often associated with complex transient spatiotemporal dynamics and energy-dependent, finite termination time (Uribe et al. dissertation). Transient dissolution of the spiral wave core is observed at the transition from suprathreshold to subthreshold light intensities[43]. It should be noted that illumination with subthreshold light intensities may also lead to wave break initiation, facilitating the onset of cardiac arrhythmias[44].

The spatial-temporal modulation of excitability, e.g., by excitability gradients and pacing, causes spiral wave drift. This effect has investigated in several studies in the context of cardiac optogenetics and subthreshold light intensity and intensity gradients[14,15,21,45]. Spiral drift is a mechanism that may contribute to finite termination times. In three-dimensional cardiac tissue, spatial gradients of light intensity result from light absorption in the tissue[46,47] and induce spiral wave drift. Depending on the incident light intensity, wall thickness, and absorption coefficient, suprathreshold light intensities near the surface and subthreshold intensities further inside the ventricular wall are possible. In this situation, both subthreshold and suprathreshold mechanisms affect the dynamics of spiral waves in the heart.

Optogenetic mouse hearts are suitable experimental model systems to validate and advance control approaches, particularly optical feedback pacing, due to the absence of stimulation artifacts otherwise common to electrical stimulation protocols. However, the present study also has several limitations. In transgenic murine hearts, we validated the efficacy of $O_{RFP}$ in terminating monomorphic and polymorphic ventricular tachycardia. These arrhythmias are associated with single stable or meandering scroll waves. Ventricular fibrillation, on the other hand, is associated with the complex dynamics of multiple scroll waves and their interaction with the heterogeneous substrate, resulting in wave breaks or pinning of waves at endogenous heterogeneities. While $O_{RFP}$ may cause multiple scroll waves to terminate progressively, it may also cause the breakup and emergence of new scroll waves[44]. Thus, the effectiveness of the termination of multiple scroll waves depends on several factors, including tissue geometry and heterogeneity, the dynamics of phase singularities (2D) and singular filaments (3D), and the mechanisms underlying their drift, interaction, and stability (creation, annihilation). The application of $O_{RFP}$ to VF is beyond the scope of this study and may be explored in future studies.

Alonso and co-workers have investigated the effect of temporal modulation of excitability on multiple phase singular filaments. Their study focuses on the impact of tissue excitability and temporal forcing on filament stability and the dynamics of scroll waves in three-dimensional excitable media[48]. They demonstrate the control of scroll waves by subthreshold non-resonant modulation of excitability and observe either the suppression or induction of scroll wave turbulence depending on forcing frequency[49].

Progress in optogenetic control of cardiac arrhythmias may impact the advancement of concepts for efficient control of cardiac arrhythmias by electrical stimulation. Several approaches have been developed to reduce the energy requirements of arrhythmia control by local or global electrical stimulation, i.e., by using multiple local electrodes or electrical fields that recruit virtual electrodes in the tissue, using open or closed-loop control strategies.

Pak and co-workers proposed the termination of ventricular fibrillation by synchronized pacing (SyncP) from local electrodes. SyncP uses one reference and several local stimulation electrodes[17]. Local stimulation currents are triggered by the activation of a reference site and delivered when the optical potential of the stimulation site is in an excitable gap. In Langendorff-perfused rabbit hearts, a lower energy requirement but higher efficacy of SyncP compared to overdrive stimulation at 90% of the VF cycle length was observed. While controlling VF with a few local pacing electrodes is remarkable, the success rates remain too low for practical applications.

Luther and Fenton and co-workers applied suprathreshold global electric field stimulation at pacing frequencies above and below the dominant frequency[7,50]. They demonstrated termination of atrial fibrillation ex vivo and in vivo (dog) with an energy reduction of 80-90% compared to single high-energy electric shocks. During far-field pacing, the electric field is applied globally, resulting in the formation of virtual electrodes and local tissue depolarization near heterogeneities in electrical conduction leading to local emission of excitation waves[51–53]. The efficacy of this open loop control approach depends on the ratio of pacing frequency and dominant frequency of the arrhythmia (Hornung et al., 2017) and the dynamics of pinning and unpinning of single[54**?** –58] and multiple spirals[59]. Buran et al. conducted a comprehensive numerical study to to explore the termination mechanisms and efficacy of periodic excitation on pacing period and number of pulses[60]. Far-field pacing has been demonstrated to effectively terminate pinned single spirals associated with tachycardia, superseding anti-tachycardia pacing[55]. Recently, further optimization led to an adaptive deceleration pacing (ADP) approach, in which a stimulation sequence is obtained from the power spectrum, slowing down the stimulation sequence from high to low pacing frequencies[61,62]. Using numerical simulations, it was shown that ADP is more robust and efficient than equidistant stimulation using overdrive or underdrive stimulation.

Uzelac and Fenton reported that low-amplitude electrical feedback stimulation may induce a transition from VF to VT and subsequently to sinus rhythm in a perfused Langendorff rabbit heart[16]. In this experiment, electric field stimulation is applied when the time since the previous stimulus exceeds a predefined time interval longer than the dominant period.

Efimov and co-workers developed a multistage algorithm combining global electric field stimulation with pacing from a local electrode. They demonstrated that this three-stage atrial defibrillation therapy terminates atrial fibrillation with significantly less energy than a single electrical shock, opening the path of low-energy defibrillation of atrial fibrillation, potentially at or below the pain threshold[63–65].

In other studies, the response of the dynamics of nonlin-

| | | Single Pulse | | Res. Feedback Pacing | | |
|---|---|---|---|---|---|---|
| NP | | 1 | 1 | 45 | 20 | $1-2$ |
| PL | ms | 10 | 100 | 20 | 20 | 20 |
| $LI_{50}$ | $\mu W/mm^2$ | 250 | 150 | 3.1 | | |
| $LI_{75}$ | $\mu W/mm^2$ | 560 | 560 | | 9.8 | |
| $LI_{100}$ | $\mu W/mm^2$ | $<1000$ | $<1000$ | | | 103.5 |
| $E_{50}$ | mJ | 0.035 | 0.21 | $0.87 \times 10^{-3}$ | | |
| $E_{tot}$ | mJ | 0.035 | 0.21 | 1 | | |
| $T_{term}$ | s | $\approx 0.1$ | $<0.1$ | 2 | 1 | 0.1 |

TABLE I. Summary. PL – pulse length, NP – mean number of pulses, $LI_{50}$ – mean light intensity per pulse at 50% success rate (SR), $E_{50}$ – mean energy per pulse at 50% SR, $E_{tot}$ – mean total energy required at 50% SR, $T_{term}$ – average time required for termination.

ear dynamical systems to weak external stimulation has been investigated[66–68]. For example, in homoclinic chaotic systems with strong fluctuations of interspike intervals, a small amount of noise has been shown to make timescales more regular by reducing the residence time in weak, unstable regions, showing phenomena including coherence resonance, noise-induced synchronization, stochastic resonance, and noise-induced phase synchronization. The response of homoclinic chaos to noise shows similarities to excitable systems, where resonance depending on signal frequency and noise intensity have been observed, motivating further research in this direction.

In summary, our results show a significant enhancement of termination efficiency at low light intensity by resonant feedback stimulation. Numerical simulations suggest that resonant drift contributes to the termination. We anticipate resonant feedback pacing, combined with advanced implantable optoelectronic devices, may open the path to efficient optogenetic control of cardiac tachyarrhthmias.

## ACKNOWLEDGMENTS

We thank Marion Kunze, Tina Althaus, and Andreas Barthel for their expertise and technical assistance in conducting this study. S.L. acknowledges support by the MPG, the German Center for Cardiovascular Research (DZHK), and SFB 1002.

[1] N. Srinivasan and R. Schilling, "Sudden cardiac death and arrhythmias," Arrhythm Electrophysiol Rev **7**, 111–117 (2018).
[2] V. Hakim and A. Karma, "Theory of spiral wave dynamics in weakly excitable media: Asymptotic reduction to a kinematic model and applications," Phys. Rev. E **60**, 5073–5105 (1999).
[3] B. Sandstede, A. Scheel, and C. Wulff, "Bifurcations and dynamics of spiral waves," Phys. Rev. E **60**, 439–478 (1999).
[4] V. Krinski, "Fibrillation in the excitable media," Problemy Kibernetiki **2**, 59–80 (1968).
[5] J. M. Davidenko, P. Kent, D. R. Chialvo, D. C. Michaels, and J. Jalife, "Sustained vortex-like waves in normal isolated ventricular muscle," Proc. Natl. Acad. Sci. USA. **87**, 8785–8789 (1990).
[6] J. M. Davidenko, A. M. Pertsov, R. Salomonsz, W. Baxter, and J. Jalife, "Stationary and drifting spiral waves of excitation in isolated cardiac muscle," Nature **355**, 349–351 (1991).
[7] S. Luther, F. H. Fenton, B. G. Kornreich, A. Squires, P. Bittihn, D. Hornung, M. Zabel, J. Flanders, A. Gladuli, L. Campoy, E. M. Cherry, G. Luther, G. Hasenfuss, V. I. Krinsky, A. Pumir, R. F. Gilmour, and E. Bodenschatz, "Low-energy control of electrical turbulence in the heart," Nature **475**, 235–239 (2011).
[8] C. M. Ambrosi, C. M. Ripplinger, I. R. Efimov, and V. V. Fedorov, "Termination of sustained atrial flutter and fibrillation using low-voltage multiple-shock therapy," Heart Rhythm **8** (2011), 10.1016/j.hrthm.2010.10.018.
[9] V. A. Davydov, V. Zykov, A. S. Mikhailov, and P. K. Brazhnik, "Drift and resonance of helical waves in distributed active media," Radiophysics and Quantum Electronics **31**, 419–426 (1988).
[10] K. I. Agladze, V. A. Davydov, and A. S. Mikhaĭlov, "Observation of a helical-wave resonance in an excitable distributed medium," ZhETF Pisma Redaktsiiu **45**, 601 (1987).
[11] V. N. Biktashev and A. V. Holden, "Design principles of a low voltage cardiac defibrillator based on the effect of feedback resonant drift," J Theor Biol **2**, 101–112 (1994).
[12] V. N. Biktashev, "Resonance and feedback strategies for low-voltage defibrillation," *Cardiac Bioelectric Therapy*, , 493–510 (2009).
[13] V. N. Biktashev and A. V. Holden, "Resonant drift of an autowave vortex in a bounded medium," Physics Letters A **181**, 216–224 (1993).
[14] S. Hussaini, *Optogenetic Control of Cardiac Arryhthmia*, Ph.D. thesis, Georg-August Göttingen University (2021).
[15] Y. X. Xia, X. P. Zhi, T. C. Li, J. T. Pan, A. V. Panfilov, and H. Zhang, "Spiral wave drift under optical feedback in cardiac tissue," Phys. Rev. E **106**, 024405 (2022).
[16] I. Uzelac and F. Fenton, "Personalized low-energy defibrillation through feedback based resynchronization therapy," Comput Cardiol **2010** (2020), 10.22489/cinc.2020.471.
[17] H. Pak, Y. Liu, H. Hayashi, Y. Okuyama, P. Chen, and S. Lin, "Synchronization of ventricular fibrillation with real-time feedback pacing: implication to low-energy defibrillation," Am J Physiol Heart Circ Physiol **6** (2003), 10.1152/ajpheart.00366.2003.
[18] T. Bruegmann, D. Malan, M. Hesse, T. Beiert, C. J. Fuegemann, B. K. Fleischmann, and P. Sasse, "Optogenetic control of heart muscle in vitro and in vivo," Nature Methods **7**, 897–900 (2010).
[19] A. B. Arrenberg, D. Y. R. Stainier, H. Baier, and J. Huisken, "Optogenetic control of cardiac function," Science **330**, 971–974 (2010), https://science.sciencemag.org/content/330/6006/971.full.pdf.
[20] E. Entcheva, "Cardiac optogenetics," American Journal of Physiology-Heart and Circulatory Physiology **304**, H1179–H1191 (2013).
[21] S. Hussaini, V. Venkatesan, V. Biasci, J. M. Romero Sepúlveda, R. A. Quiñonez Uribe, L. Sacconi, G. Bub, C. Richter, V. Krinski, U. Parlitz, R. Majumder, and S. Luther, "Drift and termination of spiral waves in optogenetically modified cardiac tissue at sub-threshold illumination," eLife **10**, e59954 (2021).
[22] R. Majumder, V. S. Zykov, and E. Bodenschatz, "From disorder to normal rhythm: Traveling-wave control of cardiac arrhythmias," Phys. Rev. Applied **17**, 064033 (2022).
[23] V. Biasci, L. Santini, G. A. Marchal, S. Hussaini, C. Ferrantini, R. Coppini, L. M. Loew, S. Luther, M. Campione, C. Poggesi, F. S. Pavone, E. Cerbai, G. Bub, and L. Sacconi, "Optogenetic manipulation of cardiac electrical dynamics using sub-threshold illumination: dissecting the role of cardiac alternans in terminating rapid rhythms," Basic Research in Cardiology **117**, 1–15 (2022).
[24] R. Burton, A. Klimas, C. Ambrosi, J. Tomek, A. Corbett, E. Entcheva, and G. Bub, "Optical control of excitation waves in cardiac tissue," Nature Photon **9**, 813–816 (2015).
[25] T. Bruegmann, P. M. Boyle, C. C. Vogt, T. V. Karathanos, H. J. Arevalo, B. K. Fleischmann, N. A. Trayanova, and P. Sasse, "Optogenetic defibrillation terminates ventricular arrhythmia in mouse hearts and human simulations," The Journal of Clinical Investigation **126**, 3894–3904 (2016).
[26] C. Crocini, C. Ferrantini, F. S. Pavone, and L. Sacconi, "Optogenetics gets to the heart: A guiding light beyond defibrillation," Progress in Biophysics and Molecular Biology **130**, 132 – 139 (2017), cardiac Mechanics and Electrics: it takes two to tango.
[27] I. Feola, L. Volkers, R. Majumder, A. Teplenin, M. J. Schalij, A. V. Panfilov, A. A. de Vries, and D. A. Pijnappels, "Localized optogenetic targeting of rotors in atrial cardiomyocyte monolayers," Circulation: Arrhythmia and Electrophysiology **10**, e005591 (2017).

[28]R. A. Quiñonez Uribe, S. Luther, L. Diaz-Maue, and C. Richter, "Energy-reduced arrhythmia termination using global photostimulation in optogenetic murine hearts," Frontiers in Physiology **9**, 1651 (2018).
[29]R. Majumder, I. Feola, A. S. Teplenin, A. A. de Vries, A. V. Panfilov, and D. A. Pijnappels, "Optogenetics enables real-time spatiotemporal control over spiral wave dynamics in an excitable cardiac system," eLife **7**, e41076 (2018).
[30]E. M. Cohen, F. L. Knapman, and L. E. Bilston, "Optogenetic control of muscles: Potential uses and limitations," **34**, 416–429, publisher: Mary Ann Liebert, Inc., publishers.
[31]H. Ryu, X. Wang, Z. Xie, J. Kim, Y. Liu, W. Bai, Z. Song, J. W. Song, Z. Zhao, J. Kim, Q. Yang, J. J. Xie, R. Keate, H. Wang, Y. Huang, I. R. Efimov, G. A. Ameer, and J. A. Rogers, "Materials and design approaches for a fully bioresorbable, electrically conductive and mechanically compliant cardiac patch technology," **n/a**, 2303429, _eprint: https://onlinelibrary.wiley.com/doi/pdf/10.1002/advs.202303429.
[32]J. Ausra, M. Madrid, R. T. Yin, J. Hanna, S. Arnott, J. A. Brennan, R. Peralta, D. Clausen, J. A. Bakall, I. R. Efimov, and P. Gutruf, "Wireless, fully implantable cardiac stimulation and recording with on-device computation for closed-loop pacing and defibrillation," Science Advances **8**, eabq7469 (2022), https://www.science.org/doi/pdf/10.1126/sciadv.abq7469.
[33]M. K. Madrid, J. A. Brennan, R. T. Yin, H. S. Knight, and I. R. Efimov, "Advances in implantable optogenetic technology for cardiovascular research and medicine," Front Physiol **5**, 1–10 (2021).
[34]V. E. Bondarenko, G. P. Szigeti, G. C. L. Bett, S.-J. Kim, and R. L. Rasmusson, "Computer model of action potential of mouse ventricular myocytes," American Journal of Physiology-Heart and Circulatory Physiology **287**, H1378–H1403 (2004).
[35]P. S. Petkova-Kirova, B. London, G. Salama, R. L. Rasmusson, and V. E. Bondarenko, "Mathematical modeling mechanisms of arrhythmias in transgenic mouse heart overexpressing tnf-$\alpha$," American Journal of Physiology-Heart and Circulatory Physiology **302**, H934–H952 (2012).
[36]J. C. Williams, J. Xu, Z. Lu, A. Klimas, X. Chen, C. M. Ambrosi, I. S. Cohen, and E. Entcheva, "Computational optogenetics: empirically-derived voltage- and light-sensitive channelrhodopsin-2 model," PLoS computational biology **9**, e1003220 (2013).
[37]V. Biktashev and A. Holden, "Resonant drift of autowave vortices in two dimensions and the effects of boundaries and inhomogeneities," Chaos, Solitons and Fractals **5**, 575–622 (1995), nonlinear Phenomena in Excitable Physiological Systems.
[38]V. Biktashev and A. Holden, "Control of re-entrant activity in a model of mammalian atrial tissue." Proc Biol Sci. **260**, 211–7 (1995).
[39]S. Morgan, G. Plank, I. Biktasheva, and V. Biktashev, "Low energy defibrillation in human cardiac tissue: a simulation study," Biophys J **96**, 1364–1373 (2009).
[40]S. Morgan, *Low-energy defibrillation using resonant drift pacing* (Thesis Ph.D., 2009).
[41]I. Biktasheva, S. Morgan, G. Plank, and V. Biktashev, "Feedback control of resonant drift as a tool for low voltage defibrillation," in *2008 Computers in Cardiology* (2008) pp. 501–504.
[42]S. Kharche, I. Biktasheva, G. Seemann, H. G. Zhang, and V. Biktashev, "Cardioversion using feedback stimuli in human atria," in *2012 Computing in Cardiology* (2012) pp. 133–136.
[43]S. Hussaini, S. L. Lädke, J. Schröder-Schetelig, V. Venkatesan, R. A. Q. Uribe, C. Richter, R. Majumder, and S. Luther, "Dissolution of spiral wave's core using cardiac optogenetics," PLOS Computational Biology **19**, e1011660 (2023), publisher: Public Library of Science.
[44]R. Majumder, S. Hussaini, V. S. Zykov, S. Luther, and E. Bodenschatz, "Pulsed low-energy stimulation initiates electric turbulence in cardiac tissue," PLoS computational biology **17**, e1009476 (2021).
[45]S. Hussaini, R. Majumder, V. Krinski, and S. Luther, "In silico optical modulation of spiral wave trajectories in cardiac tissue," Pflügers Archiv - European Journal of Physiology **475**, 1453–1461 (2023).
[46]P. Boyle, J. Williams, C. Ambrosi, *et al.*, "A comprehensive multiscale framework for simulating optogenetics in the heart. nat. commun. 4, 2370," (2013).
[47]T. Zaglia, N. Pianca, G. Borile, F. Da Broi, C. Richter, M. Campione, S. E. Lehnart, S. Luther, D. Corrado, L. Miquerol, *et al.*, "Optogenetic determination of the myocardial requirements for extrasystoles by cell type-specific targeting of channelrhodopsin-2," Proceedings of the National Academy of Sciences **112**, E4495–E4504 (2015).
[48]S. Alonso, M. Bär, and A. V. Panfilov, "Negative Tension of Scroll Wave Filaments and Turbulence in Three-Dimensional Excitable Media and Application in Cardiac Dynamics," Bulletin of Mathematical Biology **75**, 1351–1376 (2013).
[49]S. Alonso, F. Sagués, and A. S. Mikhailov, "Taming winfree turbulence of scroll waves in excitable media," Science **299**, 1722–1725 (2003), https://www.science.org/doi/pdf/10.1126/science.1080207.
[50]F. H. Fenton, S. Luther, E. M. Cherry, N. F. Otani, V. Krinsky, A. Pumir, E. Bodenschatz, and R. F. Gilmour, "Termination of Atrial Fibrillation Using Pulsed Low-Energy Far-Field Stimulation," Circulation **120**, 467–476 (2009), publisher: American Heart Association.
[51]P. Bittihn, M. Hörning, and S. Luther, "Negative Curvature Boundaries as Wave Emitting Sites for the Control of Biological Excitable Media," Physical Review Letters **109**, 118106 (2012), publisher: American Physical Society.
[52]A. Pumir, V. Nikolski, M. Hörning, A. Isomura, K. Agladze, K. Yoshikawa, R. Gilmour, E. Bodenschatz, and V. Krinsky, "Wave Emission from Heterogeneities Opens a Way to Controlling Chaos in the Heart," Physical Review Letters **99**, 208101 (2007), publisher: American Physical Society.
[53]A. Pumir and V. Krinsky, "Unpinning of a Rotating Wave in Cardiac Muscle by an Electric Field," Journal of Theoretical Biology **199**, 311–319 (1999).
[54]P. Bittihn, A. Squires, G. Luther, E. Bodenschatz, V. Krinsky, U. Parlitz, and S. Luther, "Phase-resolved analysis of the susceptibility of pinned spiral waves to far-field pacing in a two-dimensional model of excitable media," Philosophical Transactions of the Royal Society A: Mathematical, Physical and Engineering Sciences **368**, 2221–2236 (2010), publisher: Royal Society.
[55]P. Bittihn, G. Luther, E. Bodenschatz, V. Krinsky, U. Parlitz, and S. Luther, "Far field pacing supersedes anti-tachycardia pacing in a generic model of excitable media," New Journal of Physics **10**, 103012 (2008).
[56]E. Boccia, U. Parlitz, and S. Luther, "Spontaneous termination of reentrant activity under myocardial acute ischemia: Role of cellular conductivity and its relation to ischemic heterogeneities," Communications in Nonlinear Science and Numerical Simulation **48**, 115–122 (2017).
[57]E. Boccia, S. Luther, and U. Parlitz, "Modelling far field pacing for terminating spiral waves pinned to ischaemic heterogeneities in cardiac tissue," Philosophical Transactions of the Royal Society A: Mathematical, Physical and Engineering Sciences **375**, 20160289 (2017), publisher: Royal Society.
[58]S. Punacha, S. Berg, A. Sebastian, V. I. Krinski, S. Luther, and T. K. Shajahan, "Spiral wave unpinning facilitated by wave emitting sites in cardiac monolayers," Proceedings of the Royal Society A: Mathematical, Physical and Engineering Sciences **475**, 20190420 (2019), publisher: Royal Society.
[59]H. tom Wörden, U. Parlitz, and S. Luther, "Simultaneous unpinning of multiple vortices in two-dimensional excitable media," Physical Review E **99**, 042216 (2019), publisher: American Physical Society.
[60]P. Buran, M. Bär, S. Alonso, and T. Niedermayer, "Control of electrical turbulence by periodic excitation of cardiac tissue," Chaos: An Interdisciplinary Journal of Nonlinear Science **27**, 113110 (2017), publisher: American Institute of Physics.
[61]T. Lilienkamp, U. Parlitz, and S. Luther, "Taming cardiac arrhythmias: Terminating spiral wave chaos by adaptive deceleration pacing," Chaos: An Interdisciplinary Journal of Nonlinear Science **32**, 121105 (2022), https://pubs.aip.org/aip/cha/article-pdf/doi/10.1063/5.0126682/16497998/121105_1_online.pdf.
[62]T. Lilienkamp, U. Parlitz, and S. Luther, "Non-monotonous dose response function of the termination of spiral wave chaos," Scientific Reports **12**, 12043 (2022).
[63]C. M. Ambrosi, C. M. Ripplinger, I. R. Efimov, and V. V. Fedorov, "Termination of Sustained Atrial Flutter and Fibrillation Using Low Voltage Multiple Shock Therapy," Heart Rhythm **8**, 101–108 (2011).
[64]A. H. Janardhan, S. R. Gutbrod, W. Li, D. Lang, R. B. Schuessler, and I. R. Efimov, "Multistage Electrotherapy Delivered Through Chronically-Implanted Leads Terminates Atrial Fibrillation With Lower Energy Than a Single Biphasic Shock," Journal of the American College of Cardiology **63**, 40–48 (2014).
[65]W. Li, A. H. Janardhan, V. V. Fedorov, Q. Sha, R. B. Schuessler, and I. R. Efimov, "Low-Energy Multistage Atrial Defibrillation Therapy Terminates Atrial Fibrillation With Less Energy Than a Single Shock," Circulation: Arrhythmia and Electrophysiology **4**, 917–925 (2011), publisher: Ameri-

can Heart Association.
[66] A. N. Pisarchik, R. Meucci, and F. T. Arecchi, "Discrete homoclinic orbits in a laser with feedback," Phys. Rev. E **62**, 8823–8825 (2000).
[67] C. S. Zhou, J. Kurths, E. Allaria, S. Boccaletti, R. Meucci, and F. T. Arecchi, "Constructive effects of noise in homoclinic chaotic systems," Phys. Rev. E **67**, 066220 (2003).
[68] R. Meucci, S. Euzzor, F. Tito Arecchi, and J.-M. Ginoux, "Minimal Universal Model for Chaos in Laser with Feedback," International Journal of Bifurcation and Chaos **31**, 2130013 (2021).